

01 Jan 1993

Neural Network Diagnosis of Malignant Melanoma from Color Images

Fikret Erçal

Missouri University of Science and Technology, ercal@mst.edu

C. Chawla

William V. Stoecker

Missouri University of Science and Technology

Randy Hays Moss

Missouri University of Science and Technology, rhm@mst.edu

Follow this and additional works at: https://scholarsmine.mst.edu/comsci_techreports

 Part of the [Computer Sciences Commons](#)

Recommended Citation

Erçal, Fikret; Chawla, C.; Stoecker, William V.; and Moss, Randy Hays, "Neural Network Diagnosis of Malignant Melanoma from Color Images" (1993). *Computer Science Technical Reports*. 26.
https://scholarsmine.mst.edu/comsci_techreports/26

This Technical Report is brought to you for free and open access by Scholars' Mine. It has been accepted for inclusion in Computer Science Technical Reports by an authorized administrator of Scholars' Mine. This work is protected by U. S. Copyright Law. Unauthorized use including reproduction for redistribution requires the permission of the copyright holder. For more information, please contact scholarsmine@mst.edu.

NEURAL NETWORK DIAGNOSIS OF MALIGNANT
MELANOMA FROM COLOR IMAGES

F. Ercal, A. Chawla, and W. V. Stoecker

CSC-93-04

Department of Computer Science
University of Missouri-Rolla
Rolla, MO 65401

Neural Network Diagnosis of Malignant Melanoma From Color Images‡

F. Ercalt, A. Chawla, and W. V. Stoecker

Department of Computer Science

University of Missouri - Rolla

Rolla, MO 65401

R. H. Moss

Department of Electrical Engineering

University of Missouri - Rolla, Rolla, MO 65401

Abstract

Malignant melanoma is the deadliest form of all skin cancers. Approximately 32,000 new cases of malignant melanoma were diagnosed in 1991, with approximately 80 percent of patients expected to survive five years [1]. Fortunately, if detected early, even malignant melanoma may be treated successfully. Thus, in recent years, there has been a rising interest in the automated detection and diagnosis of skin cancer, particularly malignant melanoma [2]. In this paper, we present a novel neural network approach for the automated separation of melanoma from three other benign categories of tumors which exhibit melanoma-like characteristics. Our approach is based on devising new and discriminant features which are used as inputs to an artificial neural network for classification of tumor images as malignant or benign. We have obtained promising results using our method on real skin cancer images.

1 Introduction

Dermatology imaging researchers believe that diagnosis of skin tumors can be automated based on certain physical features and color information that are characteristic of the different categories of skin cancer. Diagnosis of malignant melanoma is a difficult task since other skin cancers have similar physical characteristics. In many cases, dermatologists must perform a biopsy (a laboratory medical procedure) to ascertain whether a tumor is malignant or benign.

†Intelligent Systems Center, University of Missouri-Rolla, Rolla MO 65401

‡This work was supported in part by the National Science Foundation under SBIR Phase II award number ISI-8521284 and the Intelligent Systems Center of the University of Missouri-Rolla

Since this is a costly procedure, alternative early detection techniques are being sought to for rapid inexpensive skin cancer screening. In this study, we use color images of skin tumors, image processing techniques, and an artificial neural network to distinguish melanoma from other benign pigmented tumors: dysplastic nevi, intradermal nevi and seborrheic keratoses. We first define those features that are expected to distinguish melanoma from the three other skin tumors, and train an artificial neural network with these features in an attempt to classify the tumor type as melanoma or not.

The characteristics of malignant melanoma and three categories of benign tumors which are difficult to distinguish from melanoma are outlined below. These descriptions are brief and inherently inaccurate. They apply to only the most typical members of a diagnostic group.

Malignant Melanoma : Malignant melanoma is named for the cell from which it presumably arises, the melanocyte. Melanocytes are the skin cells which produce the dark protective pigment called melanin, a natural sunscreen. Melanoma cells usually continue to produce melanin, which accounts for the cancers appearing in mixed shades of tan, brown and black (variegated coloring). Melanoma has a tendency to metastasize (spread), hence early detection and treatment are essential.

Friedman et al. have enumerated the mnemonic "ABCD" to describe early malignant melanoma [3]:

1. **Asymmetry** - One half of the tumor does not match the other half.
2. **Border Irregularity** - The edges are ragged, notched, blurred.
3. **Color** - Pigmentation is not uniform. Shades of tan, brown and black are present. Dashes of red, white and blue add to the mottled appearance.
4. **Diameter** - greater than 6 mm and growing.

Dysplastic Nevi (dys nevi) : Moles, or nevi, are tan brown spots on the skin that result from a clustering of melanocytes. Certain unusual moles called dysplastic nevi are likely to undergo changes leading to melanoma. Scientists believe that individuals with dysplastic nevi, especially those from families with multiple cases of melanoma, represent one group of people who are more likely to develop melanoma. It is important to remember that, although the dysplastic nevus is the kind of mole most likely to undergo malignant changes, most dysplastic nevi do not become malignant.

The National Cancer Institute [4] has outlined the following characteristics for the detection of dysplastic nevi, lesions that may occur in both familial and non-familial settings, and are associated with a higher risk of malignant melanoma:

1. Color - Mixture of tan, brown, black and red/pink.
2. Shape - Irregular Borders that may include notches. May fade into surrounding skin and include a flat portion level with the skin.
3. Surface - Smooth , slightly scaly, or have a rough pebbly appearance.
4. Size - often larger than 5mm and sometimes larger than 10mm.

Intradermal Nevi (Idn) : These are benign tumors. Idn are most common in children and young adults and may be tan, brown, flesh or pink. These are commonly called moles and may be hairy. Dermatologists agree upon the following characteristics of idn (modified from [4]):

1. Color - Flesh colored, pink, may be tan or brown.
2. Shape - Round or oval, may fade gradually into the surrounding skin.
3. Surface - Often smooth, sometimes papillomatous, and raised. Skin markings are present when examined with a hand lens.
4. Size - Usually less than 6mm in diameter.

Seborrheic Keratoses (sk) : These are benign tumors found in older persons, with patients usually older than forty. They are benign growths of the epidermis (outer layer of the skin) with the following clinical characteristics (modified from [4]):

1. Color - Tan to brown, may be fleshy or pink, darker in persons with darker skin.
2. Shape - Borders often oval or round but may be irregular, often sharply demarcated but in fair persons fading gradually into surrounding skin.
3. Surface - Rough, verrucous, sometimes with keratin plugs. Skin markings are almost always enhanced, even if the surface is not rough. The raised surface and frequently sharp border lead to the appellation "stuck-on". The tan to yellowish color combined with the stuck-on appearance is sometimes called "tallow-drop".
4. Size - 3mm - 30mm or more, usually 5-15 mm.

5. Location - Seborrheic keratoses are usually located on the face, neck and trunk.

These descriptions indicate that melanoma and the above categories of benign tumors differ slightly in their physical characteristics and colors. If any automated approach is to succeed in diagnosing melanoma, a collection of these features rather than a single feature needs to be used in order to obtain a satisfactory classification of the tumor images belonging to one of these categories. Indeed, this fact is also reflected by Figures 1 and 2, obtained after processing and examining 326 digital images of skin growths of the above mentioned categories. These figures show some statistical data on the distribution of percentages of tumors within each class with respect to irregularity and asymmetry. Figure 1 suggests that the irregularity index (to be explained later) alone is not sufficient in diagnosing melanoma since many benign tumors have irregularity indices which are as high as those for melanoma. Similarly, Figure 2 indicates that percent asymmetry (obtained by overlapping the two halves of a tumor along the best axis of symmetry and dividing the nonoverlapping area differences of the two halves by the total area of the tumor) also does not give a satisfactory separation between melanoma and other benign tumors.

When diagnosing skin cancer, dermatologists base their clinical diagnostic decisions on experience as well as on complex inferences and extensive pathophysiological knowledge. Such experience cannot be condensed into a small set of relations, and this limits the performance of algorithmic approaches of many clinical tasks. The breadth of clinical knowledge is an obstacle to the creation of symbolic knowledge bases comprehensive enough to cope with diverse exceptions which occur in practice. Experience-based learning is the property of artificial neural networks which make them ideal for diagnostic applications such as the one above. Using the indices described above, as well as color information, a neural network should be able to learn and gain experience about the malignant melanoma diagnosis problem. The ability to select pertinent features for a particular problem on their own is an edge which neural networks possess over expert systems when solving such diagnosis problems. They are limited, of course, to those features that experimenters select.

In the following section, we give a brief introduction of artificial neural networks as pattern classifiers and explain the training/testing approach for classification. In Section 3, we describe our approach to diagnosing the melanoma tumors and the selection and derivation of the features used for this purpose. Experimental results and discussion are given in Section 4.

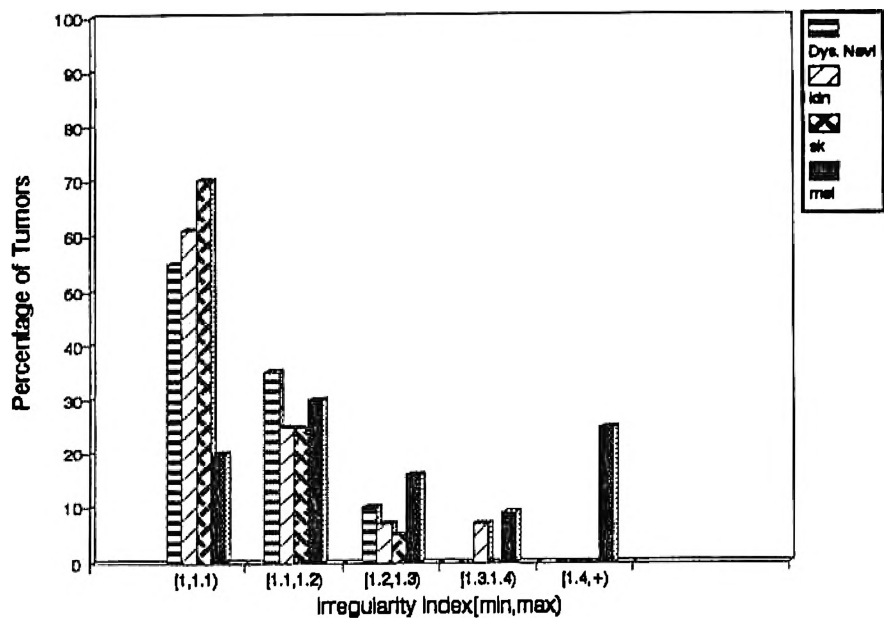


Figure 1: Percentages of tumors having different irregularity indices

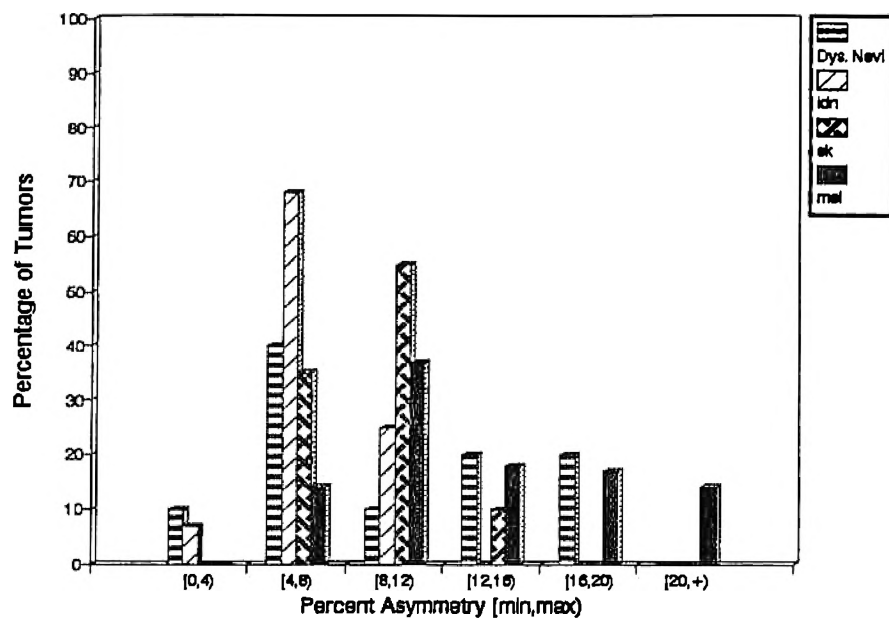


Figure 2: Percentages of tumors having different asymmetry indices

2 Artificial Neural Networks As Pattern Classifiers

In recent years, neural networks have been used as pattern classifiers in medical diagnosis [5], speech [6] and pattern recognition [7], and artificial intelligence applications. This trend has even accelerated by the availability of high speed computers with large amounts of processing power and memory. There is an increasing interest in the use of neural networks to solve a variety of problems in many areas of medicine and engineering. Adaptive non-parametric neural-net classifiers work well for many real world problems. These classifiers frequently provide reduced error rates when compared to more conventional statistical approaches and are a powerful and flexible means for mapping a fixed number of inputs into a set of discrete classes. These characteristics make artificial neural networks a strong candidate for diagnostic problems where a set of symptoms is mapped to a set of possible diagnostic classes. In our research, we are motivated by the desire to classify skin tumors as malignant or non-malignant from color photo slides of the tumors and to further explore how we can add learning to this diagnosis process in order to automatically classify the skin tumors correctly.

In our application, it is necessary to classify digital images of tumors into a small number of fixed categories. Feedforward neural networks are ideally suited for this purpose. The type of network that best fits our diagnosis application is a multilayered feedforward neural network trained using the generalized delta rule (backpropagation training algorithm). Backpropagation neural networks fall into the group of hyperplane classifiers [8]. Nodes in this network typically form a weighted sum of the inputs and pass this sum through a sigmoidal nonlinearity. Other nonlinearities including high-order polynomials of the inputs can also be used. The network is trained with supervision using a gradient-descent training technique, called backpropagation, which minimizes the squared error between actual outputs of the network and the desired outputs. The backpropagation classifier has been successfully used for many pattern recognition applications including speech recognition [6], bone fracture healing assessment [9], and handwriting recognition [10]. In our system, one hidden layer was used based on the fact that training times were shorter and it exhibited a satisfactory training performance among several network configurations with which we had experimented. It was also shown, in a recent study, that arbitrary decision regions can be approximated by multi-layer perceptrons with only one hidden layer [8].

Supervised learning is achieved via the training/testing paradigm. Two statistically in-

dependent, disjoint sets are used for the training and test sets to allow unbiased results to be obtained on the test set. The network is trained and tested repeatedly with different random subsets of the input data and by taking averages on the results obtained. In order to generate the best classification network possible, the size of the training set should be maximized; on the other hand, to improve the confidence level in the results as an estimate of future performance, the size of the test set should be maximized. This suggests an equal size for training and testing sets. However, various sizes of training and testing sets were preferred in our study in order to provide a wider spectrum of results and hence, to allow for observation of trends in the data.

Artificial neural networks, in general, have some important properties which are useful in recognizing noisy patterns. When the training set contains noisy or inconsistent samples, during the learning phase, the network extracts the central tendency (or prototype) of the set. After learning, the network can generalize, giving correct responses even in the presence of patterns that are not included in the training set. This is very important in our application since we are dealing with digital images of tumors which may have noise in the form of reflections of electronic flash units, shadows, hair etc. Hence it is possible that some of the features we extract from images may present irrelevant variability due to this noise. The network is generally insensitive to this form of variability in the input, which is commonly encountered in practical applications.

3 Selection of Features for Diagnosing Melanoma

Diagnostic applications require a selection of features that must be tailored separately for each problem domain. The features selected should contain enough information to distinguish between classes while being insensitive to irrelevant variability in the inputs. We defined 14 features that we believe to be well discriminative between images belonging to malignant melanoma and the three benign tumors of interest here. All of the 14 features that were identified to be useful in the diagnosis required detection of the border of the tumor in the color image. Boundary detection is a non-trivial process and it is explained in detail in [11, 12]. After the boundary of the tumor area is determined, the next step is to compute the indices corresponding to each feature needed for diagnosis. This section provides a brief description of the selected features as well as the methodology used to extract them from the color skin

images.

Irregularity Index

Malignant melanoma is characterized by the irregularity in its tumor border. For this study, we measured irregularity by an index $I = \frac{P^2}{4\pi A}$ where, P = perimeter of the tumor in pixels and A = area of the tumor in pixels. The irregularity index for a circle is one (perfectly regular). Most melanomas have a high irregularity index, i.e., they have an irregular shape. However, there is a significant percentage of other tumors with high irregularity indices. Hence, this feature alone is not sufficient to discriminate melanoma from benign types of tumors.

Percent Asymmetry

Asymmetry is another characteristic of malignant melanoma. Asymmetry is computed by finding an axis that is closest to the axis of symmetry of the tumor (i.e., the axis around which, if the tumor is folded into half, there is maximum overlap of the two halves). Then percent asymmetry is computed by overlapping the two halves of a tumor along the best axis of symmetry and dividing the nonoverlapping area differences of the two halves by the total area of the tumor. We found that 86% of the melanomas in our database of images have an asymmetry percentage above 8 percent, whereas this figure is 50%, 25% and 65% for the dysplastic nevi, sk and idn respectively.

Color

One of the most predictive features in identification of malignant melanoma is *variegated coloring (VC)* [1, 13]. Dermatologists define variegated coloring as the swirling together of tan, brown, red and black giving the tumor a varied coloring. Such variegation in color implies a high variance in red (R), green (G), and blue (B) color components. Therefore, out of 12 color features, three of them are selected to be the variances in the R, G, and B color planes. Since dysplastic nevi may also turn into melanoma they also have high variances in these planes but the other benign tumors have lower variances in the RGB planes (they do not exhibit variegated coloring). In addition to variances, relative chromaticity of tumors (in RGB planes) are also added to the feature list since these features are important in discriminating melanoma from sk and idn. The relative chromaticity is defined as the normalized value of that color in the tumor area subtracted from the normalized value for the color in the background.

For example the relative chromaticity of red is defined as:

$$R_{red} = \frac{r_t}{r_t + b_t + g_t} - \frac{r_{bg}}{r_{bg} + b_{bg} + g_{bg}}$$

where r_t , g_t , and b_t denote tumor RGB components and r_{bg} , g_{bg} , and b_{bg} denote background RGB components. The selection of this feature is motivated by the relative color concept, useful in differentiating between different tumor colors [13]. The relative color was defined as the color difference vector, i.e. difference in the color space between tumor and the background, or normal flesh. Reasons behind the development of a relative color concept are stated in [13] as follows: 1) to equalize any variations caused by lighting, photography/printing, or digitization process, 2) to equalize variations in normal skin color between individuals, and 3) the human visual system works on a relative color system.

Previous studies in diagnosing melanoma [13] with an expert system indicate that spherical color space coordinates gave better diagnosis results than the RGB, CIE or IHS color spaces. Therefore, we also added these indices into our set of input features. The equations to transform from (R, G, B) to spherical coordinates are given by [13]:

$$L = \sqrt{R^2 + G^2 + B^2} \quad Angle A = \cos^{-1} \left[\frac{B}{L} \right] \quad Angle B = \cos^{-1} \left[\frac{R}{L \times (\sin(Angle A))} \right]$$

This transformation splits the color space into a two-dimensional color space, represented by two angles, Angle A and Angle B; and a one dimensional intensity (brightness) space, represented by the vector length L. To compute Length, Angle A and Angle B for each tumor image we found Length, Angle A and Angle B for each of the pixels in the tumor and took an average of them.

From the viewpoint of color clustering, it is desired that the image be represented by color features which constitute a space possessing uniform characteristics such as the (L^* , a^* , b^*) color coordinate system [14]. Since sk's and idn's are brighter in color (closer to white) than melanoma and dysplastic nevi, they have distinct values in this color space. Dermatology imaging researchers also believe that this space may be useful in distinguishing melanoma from dysplastic nevi due to small differences in lightness, hue and chroma between dysplastic nevi and melanoma (according to dermatologists dysplastic nevi are brighter and have less blue, i.e. more relative red components). In our research, lightness, hue and chroma are computed for each point in the tumor using the formulas given in [14] and then an average is taken for all the pixels in the tumor.

4 Diagnosis of Malignant Tumors Using a Neural Network

For the research reported here, discriminant features explained above were extracted from 326 digital images of skin cancer. All these images were 512 x 512 pixel color images with 24 bits per pixel (8 bits for each R, G and B planes). Ninety-six images were in the malignant melanoma category and there were 111 images of dysplastic nevi (dys nevi), 58 intradermal nevi (idn) and 61 seborrheic keratoses (sk).

4.1 Neural Network Implementation

A feedforward artificial neural network with 14 inputs (see Table 1) and one output (indicating whether the tumor is malignant melanoma or not) was used and trained using the backpropagation rule. Commercial neural network software, called NeuralWorks, was used on a 486/33Mhz PC platform.

Table 1: List of Input Features Used to Train and Test the Neural Network

INPUT DESCRIPTION	NUMBER OF INPUTS
Irregularity Index	1
Percent Asymmetry	1
R, G, and B color variances	3
Relative Chromaticity (R,G,B)	3
Spherical color coordinates (L,A,B)	3
(L*, a*, b*) color coordinates	3

One major characteristic of backpropagation classifiers is long training times. Training times are typically longer when complex decision regions are required and when networks have more hidden layers. One way of solving this problem is to use few hidden layers. In this study, only one hidden layer was used based on the fact that it performed reasonably well among several network configurations with which we had experimented and also produced fast results. Typical training times varied between 40-60 minutes. Another technique that we have used in reducing the training time is randomization of the presentation of the order of the training examples by using a "shuffle and deal" randomization scheme. Other techniques which are effective in reducing training time with some applications are to update weights after presenting each training example instead of after cycling through all the examples.

Training of the network was continued with several epochs of the training set until the root mean square error of the output was below 0.05. Testing was done and the success rates for the correct diagnosis of melanoma as melanoma and non-melanoma as non-melanoma were recorded. Results were obtained for training/testing percentages of 20/80, 30/70, 40/60, 50/50, 60/40, 70/30, and 80/20.

4.2 Experimental Design and Test Results

The experiments were designed to test the effectiveness of the input features in discriminating the melanoma images from the others. Two sets of experiments were conducted, each repeated twice; once with dysplastic nevi included and another time with dysplastic nevi excluded, resulting in a total of four experiments. Those experiments with dysplastic nevi included used a total of 210 (211 in one case) images (96 melanomas, 43 dysplastic nevi, 30 idn, and 41 sk) while those with dysplastic nevi excluded used 216 images (96 melanomas, 58 idn, and 62 sk) for training plus testing. The primary focus for training was to be able distinguish melanoma from benign tumors. Experimentation has shown that the total number of melanomas needed to be close to 50% of the whole population in order to obtain good diagnostic results. The reason for the varying numbers used for each class is that we tried to maximally utilize the images available in the database for training and testing while, at the same time, keeping a good balance of different types of tumor images. For both experiments, 96 melanoma images were used and the total number of non-melanoma images were kept within a margin not exceeding 56% of the whole population. When $X\%$ of images was used for training, the remaining images ($100-X\%$) were used for testing. Each class contributed the same percentage of their total number to the training and test sets. Experiments differed from one another by the set of input features used. The first set of experiments was conducted with the 14 input features originally described and tested the effectiveness of these features in the diagnosis of melanoma. The second set of experiments were designed to test the effects of the use of different film types in the diagnosis process. In these experiments, to offset the effects of the different films used, spherical color space coordinates and (L^*, a^*, b^*) color coordinates were removed from the input set leaving only those color features related to the relative color concept (color variances and the relative color). Hence, only eight input features were used in this phase. The results of these experiments are summarized and plotted in the following paragraphs.

4.2.1 Experiments 1a and 1b

Experiment 1a was conducted with all four classes, melanoma, idn, dys nevi, and sk, while dysplastic nevi images were removed from experiment 1b. A total of 211 and 216 images were used altogether for training plus testing for experiments 1a and 1b, respectively, with 14 input features supplied per image. Results are plotted in figures 3a and 3b. In experiment 1a, for training percentages exceeding 60%, melanomas are diagnosed with close to 90% success rate. The sks and idn's are always above 90 percent for training percentages on or above 40%. The dysplastic nevi are however quite inconsistent and vary between a low of 50 and a high of 85 percent. We believe this is due to the fact that dysplastic nevi are precursors of melanoma and they possess the same variegation of coloring as melanoma tumors. In experiment 1b, the results improve appreciably (Figure 3b) for melanoma with successful diagnosis rate not below 92% for any case, peaking at 96%. The other two categories did not exhibit any significant changes and were diagnosed with success rates of 100% for training sizes above 60 percent, with the exception of idn showing a poor performance for the training percentages of 40% or below. This result supports the original observation that dysplastic nevi are precursors of melanoma and they possess the same variegation of coloring as melanoma tumors. Hence, elimination of the dysplastic nevi images from the training set made the classification job easier for the network and the number of false negatives were reduced considerably. As a result, the overall performance (the curve with a solid black icon) was boosted considerably (to a 98% success rate with a training set size of 80%).

4.2.2 Experiments 2a and 2b

The same procedure used for experiment 1 was repeated for this set of experiments except that 8 input features were used instead of 14. The goal was to test the effect of the types of film used. In our image database, all the melanoma and dysplastic nevi slides were Ektachrome while a majority of the sk and idn slides were Kodachrome. To offset the effect of the different film types used, absolute color components in the input, namely spherical color space coordinates and (L^*, a^*, b^*) color coordinates, were removed from the input set leaving only those color features related to the relative color concept (color variances and the relative color). Hence, only eight input features were used in this phase. Obviously, elimination of all the absolute color information from the input is expected to cause the success rate to go down due to

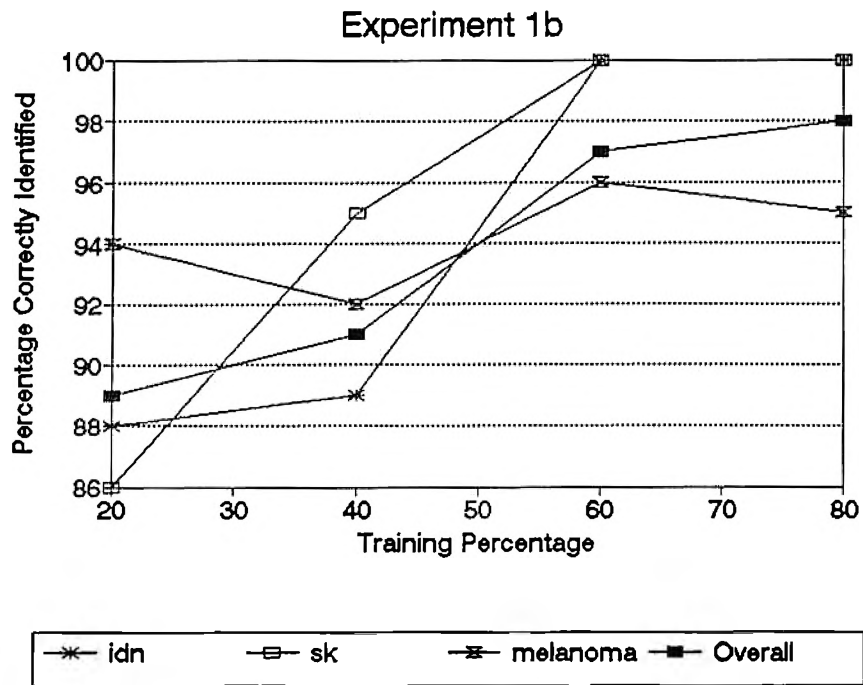
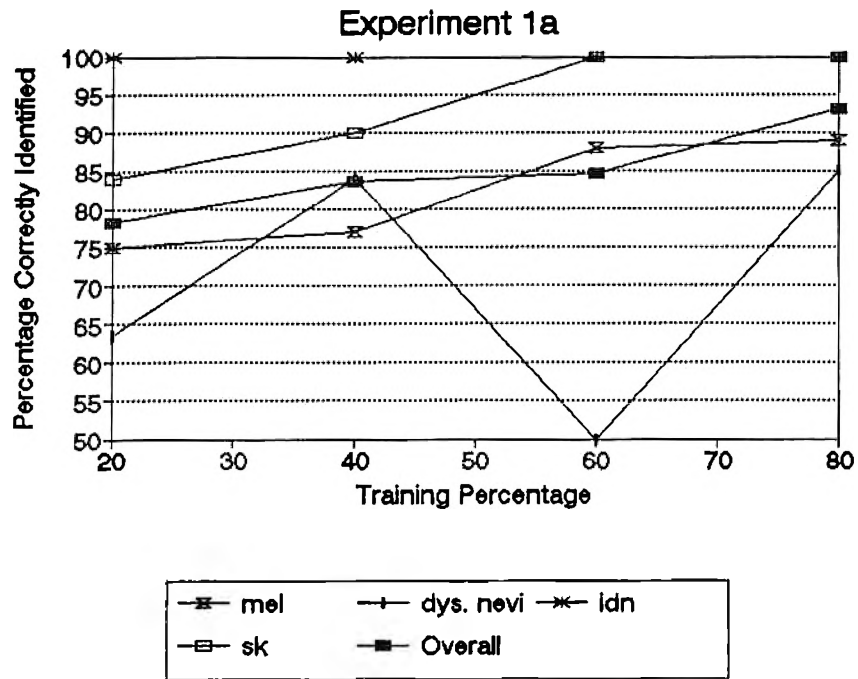


Figure 3: Neural network diagnostic results obtained with 14 input features: asymmetry, irregularity, and 12 color features. a) dysplastic nevi images included, b) dysplastic nevi images excluded

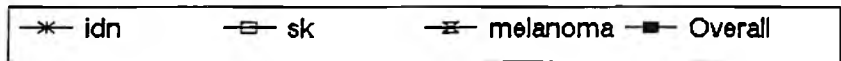
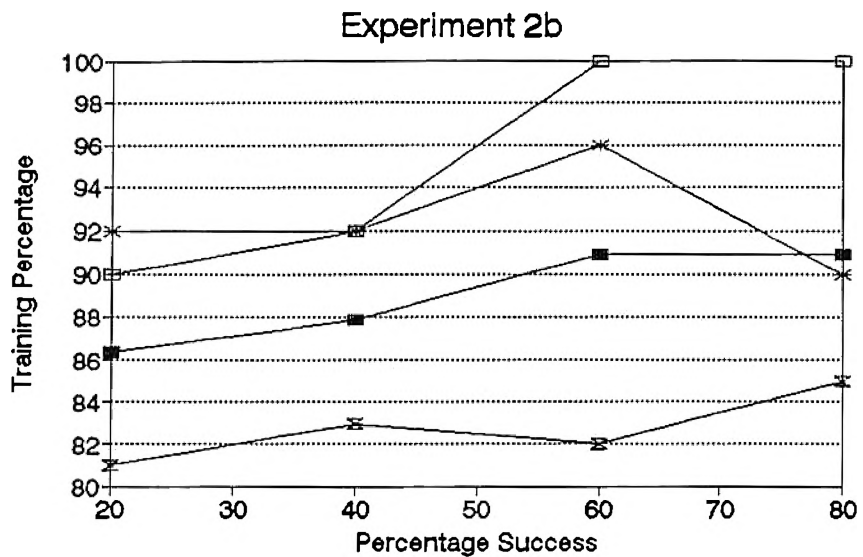
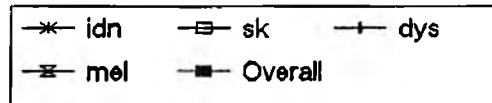
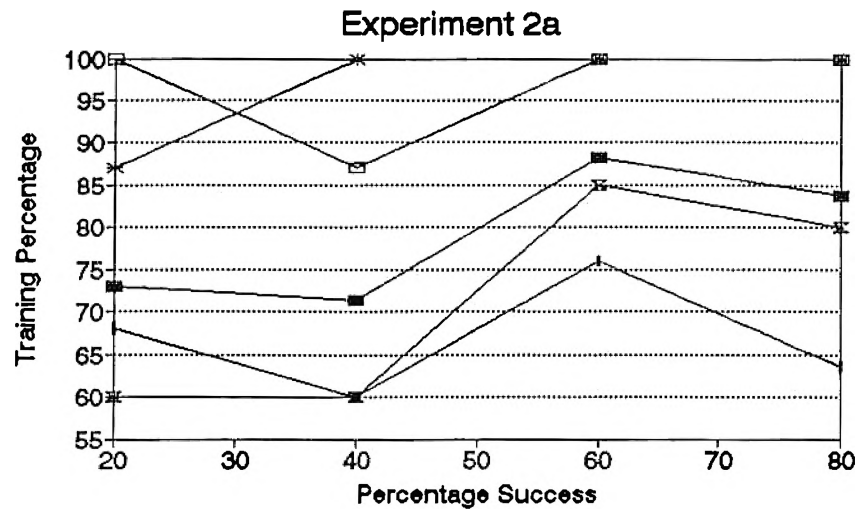


Figure 4: Neural network diagnostic results obtained with 8 input features: asymmetry, irregularity, and 6 relative color features. a) dysplastic nevi images included, b) dysplastic nevi images excluded

the degradation of the discriminant features in the input. However, we should not expect a significant change from the previous results, which would otherwise be interpreted as due to the film type. As illustrated by the plots in Figures 4a and 4b, the change in corresponding success rates is not large enough to raise concerns about the effect of film type on the results. However, it was observed that the melanoma success percentages in Exp. 2b were relatively lower than those of experiment 1b (~10% drop). This result can be explained due to the importance of absolute color information in the input. Absolute color information is important in the diagnostic process particularly from the viewpoint of color clustering (shades of tan, brown and black, dashes of red, white and blue are signs of malignancy) and brightness information of tumors in the form of the brightness vector in the spherical transform domain. Hence, including as much color information about tumors as possible helps the neural network in diagnosis of the malignant and nonmalignant tumors.

5 CONCLUSIONS

A fast and effective method to separate malignant melanoma from other types of benign tumors is becoming increasingly needed due to the fact that malignant melanoma incidence has risen dramatically in recent years and early detection can save thousands of lives each year. In this study, we attempted to diagnose melanoma from color skin images using an artificial neural network. For this purpose, a set of features to distinguish melanoma from three other types of benign tumors was defined and methods to measure these features from digitized color slides were described. Overall, diagnostic results were found to be very promising and as high as 97% accuracy in detecting malignant melanoma is achieved using training data sets of reasonable size (see experiment 1b). As a result of this study, the following results are confirmed experimentally: a) Color characteristics of tumors play a crucial role in the diagnosis process, b) tumor asymmetry and border irregularity are two important diagnostic features for distinguishing malignant melanoma from benign tumors such as seborrheic keratoses, dysplastic nevi, and intradermal nevi, c) malignant melanoma and dysplastic nevi images exhibit some similarities and therefore testing for tumor malignancy in the absence of dysplastic nevi images gives better diagnostic results. This is confirmed by the second part (b) of each experiment.

References

- [1] R. J. Friedman, D. S. Rigel, M. K. Silverman, A. W. Kopf and K. A. Vossaert, "Malignant Melanoma in the 1990s: The Continued Importance of Early Detection and the Role of Physician Examination and Self-Examination of the Skin," *Ca-A Journal for Clinicians*, pp. 201-226, July/August 1991.
- [2] W. V. Stoecker and R. H. Moss, "Editorial: Digital Imaging in Dermatology," *Computerized Medical Imaging and Graphics*, Vol. 16(3), pp. 145-150, May-June 1992.
- [3] R. J. Friedman, D. S. Rigel, A. W. Kopf, "Early Detection of Malignant Melanoma: The Role of Physician Examination and Self-Examination of the Skin," *Ca-A Cancer Journal for Clinicians*, Vol. 35(3): pp. 130-151, 1985.
- [4] National Cancer Institute, *What you need to know about Dysplastic Nevi*, NIH Publication 91-3133, Reprinted October 1990.
- [5] R. Poli, S. Cagnoni, R. Livi, G. Coppini, G. Valli, "A Neural Network Expert System for Diagnosing and Treating Hypertension," *IEEE Computer*, Vol. 24, No. 3, pp. 64-71, March 1991.
- [6] R. P. Lippmann, "Review of Neural Networks For Speech Recognition," *Neural Comp.*, Vol. 1(1), pp. 1-38, 1989.
- [7] T. Kohonen, G. Barna, and R. Chrisly, "Statistical Pattern Recognition with Neural Networks: Benchmarking Studies," *Proc. of IEEE Annual Int'l. Conf. on Neural Networks*, Vol.I, San Diego, pp. 61-68, July 1988.
- [8] Richard P. Lippman, "Pattern Classification Using Neural Networks," *IEEE Communications Magazine*, Vol. 27, No. 11, pp. 47-64, Nov. 1989.
- [9] J. J. Kaufman et al., "A Neural Network Approach for Bone Fracture Healing Assessment," *IEEE Engineering in Medicine and Biology*, Vol. 9, pp. 23-30, Sept. 1990.
- [10] G. L. Martin and J. A. Pittman, "Recognizing Handprinted Letters and Digits," *Proc. IEEE Conf. Neural Information Processing Systems*, San Mateo, CA, pp. 405-414, Nov. 1990.
- [11] J. E. Golston, R. H. Moss, W. V. Stoecker, "Boundary Detection in Skin Tumor Images: An Overall Approach and a Radial Search Algorithm," *Pattern Recognition*, Vol. 23, no.11, pp. 1235-1247, 1990.

- [12] F. Ercal, M. Moganti, W. V. Stoecker, and R. H. Moss, "Boundary Detection and Color Segmentation in Skin Tumor Images," conditionally accepted for publication in *IEEE Transactions on Medical Imaging*, 1993.
- [13] S. E. Umbaugh, *Computer Vision in Medicine: Color Metrics and Image Segmentation Methods for Skin Cancer Diagnosis*, Ph.D. Dissertation, Elect. Eng. Dept., University of Missouri-Rolla. UMI Dissertation Services, Ann Arbor, Michigan, 1990.
- [14] M. Celenk, "A Color Clustering Technique for Image Segmentation," *Computer Vision, Graphics and Image Processing*, Vol. 52, pp. 145-170, 1990.

LIST OF FIGURE AND TABLE CAPTIONS USED IN THE MANUSCRIPT

Figure 1: Percentages of tumors having different irregularity indices

Figure 2: Percentages of tumors having different asymmetry indices

Figure 3: Neural network diagnostic results obtained with 14 input features: asymmetry, irregularity, and 12 color features. a) dysplastic nevi images included, b) dysplastic nevi images excluded

Figure 4: Neural network diagnostic results obtained with 8 input features: asymmetry, irregularity, and 6 relative color features. a) dysplastic nevi images included, b) dysplastic nevi images excluded

Table 1: List of Input Features Used to Train and Test the Neural Network